Front. Electr. Electron. Eng. China (2006) 4: 380–384
DOI 10.1007/s11460-006-0073-5

RESEARCH ARTICLE

JIANG Tie-zheng, CHEN Chen, CAO Guo-yun

Nonlinear optimal predictive controller for static var compensator to improve power system damping and to maintain voltage

Abstract The main objectives of this paper are to simultaneously improve power system damping and to maintain voltage at the static var compensator (SVC) location bus simultaneously. A new controller for SVC with closed-form analytic solution nonlinear optimal predictive control (NOPC) law was presented. The controller does not require online optimization and the huge calculation burden can be avoided, so that the demand of real-time control can be satisfied. In addition, there are only two design parameters, which are the predictive period and control order; so it is easy to implement and test in practical use. Simulation results have shown that the controller can not only attenuate power system oscillation effectively but can also maintain voltage at the SVC bus location.

Keywords SVC, NOPC, power system, damping, closed-form analytic solution control law

1 Introduction

With the development of electronic technologies, SVCs have been widely used in the modern power systems and have provided rapid control of the reactive power. So they can keep voltages at or near a constant level, enhance the power transfer capability and improve the power system transient stability [1]. It is well known that the SVC with only pure voltage regulation does not provide adequate damping, since the primary task of the pure voltage regulation is to control voltage [2]. Many research results have demonstrated that SVCs do not have the ability to produce a significant amount of damping; it may even weaken damping under traditional pure voltage control scheme [2, 3]. So it is valuable to design a new SVC controller to improve power system damping and to maintain voltage simultaneously. In fact, a great deal of progress on the investigation of the SVC control strategy has been made [4–6].

Predictive control provides a promising method for linear and nonlinear systems, which is extremely successful in the field of industrial applications. The core of predictive control is online shift performance optimization in terms of a given performance index. It turns the open-loop optimization into the closed-loop optimization during the process of control through repeated online optimization and feedback correction, It can also achieve timely correction of the uncertainty effect of the system. Therefore, its adaptiveness to intricate conditions is superior to traditional optimal control methods. However, for nonlinear systems, the numerical computation burden of online optimization is huge and the demand of real-time control may not be satisfied [7]. In this paper, based on nonlinear optimal predictive control theory, some feedback signals, power angle δ and angular speed deviation $\Delta\omega$ are introduced. A novel design for the SVC damping controller that is superposed upon its voltage regulation loop with closed-form analytical solution control law is presented. The highlight of this method is that the controller does not require online optimization and the huge calculation burden can be avoided, and the stability of the closed-loop system is guaranteed. Simulation results have shown that the controller is effective.

Translated from *Journal of Hunan University* (*Natural Sciences*), 2005, 32(5): 41–45 (in Chinese)

JIANG Tie-Zheng(✉)
Department of Electrical Engineering,
Changsha University of Science and Technology,
Changsha 410076, China
E-mail: jiangtiezheng@hotmail.com

CHEN Chen, CAO Guo-Yun
School of Electronic Information and Electrical Engineering,
Shanghai Jiao Tong University, Shanghai 200240, China

2 A design method of nonlinear optimal predictive controller

2.1

Consider the nonlinear system

$$\begin{aligned} \dot{\boldsymbol{x}}(t) &= \boldsymbol{f}(\boldsymbol{x}(t)) + \boldsymbol{g}(\boldsymbol{x}(t))\boldsymbol{u}(t) \\ \boldsymbol{y}(t) &= \boldsymbol{h}(\boldsymbol{x}(t)) \end{aligned} \tag{1}$$

where $\boldsymbol{x} \in \mathbb{R}^n, \boldsymbol{u} \in \mathbb{R}^m$ and $\boldsymbol{y} = [y_1, y_2, \cdots, y_m]^{\mathrm{T}} \in \mathbb{R}^m$ are the state, control and output vectors, respectively. Some assumptions are given to the nonlinear Eq. (1):

A1: The zero dynamics is stable.

A2: All states are available.

A3: The output $\boldsymbol{y}(t)$ and the reference signal $\boldsymbol{w}(t)$ are sufficiently many times continuously differentiable with respect to t.

To avoid the difficulty of solving partial differential equations for nonlinear optimal control, nonlinear optimal predictive control adopts a shift closed-loop optimal control algorithm. It is advantageous to determine the next control sequence by online performance index optimization so that the process output $\boldsymbol{y}_i(t)$ rallies a set-point trajectory $\boldsymbol{W}(t)$ in the future without tracking error. Therefore, the receding-horizon performance index adopted is given by:

$$J = \frac{1}{2}\int_0^T (\hat{\boldsymbol{y}}(t+\tau) - \hat{\boldsymbol{W}}(t+\tau))^{\mathrm{T}} (\hat{\boldsymbol{y}}(t+\tau) - \hat{\boldsymbol{W}}(t+\tau))\,\mathrm{d}\tau \quad (2)$$

where T is predictive period, $\hat{y}(t+\tau)$ is predictive outputs in the predictive period, $\hat{\boldsymbol{W}}(t+\tau)$ is set-point trajectory in the predictive period.

2.2 Output prediction

The moving time frame is predicted by the Taylor series expansion. If relative degree [8] of the Eq. (1) is ρ, when the control order is chosen as r, to make the rth derivative of the control signal appear [9], the order of Taylor expansion of the output $\hat{\boldsymbol{y}}(t+\tau)$ must be at least $\rho + r$. Repeated differentiation up to $\rho + r$ times of the output $\hat{\boldsymbol{y}}(t)$ with respect to time, together with respected substitution of Eq. (1) gives

$$\hat{\bar{\boldsymbol{Y}}}(t) = \begin{bmatrix} \hat{\boldsymbol{y}}^{[0]} \\ \hat{\boldsymbol{y}}^{[1]} \\ \vdots \\ \hat{\boldsymbol{y}}^{[\rho]} \\ \hat{\boldsymbol{y}}^{[\rho+1]} \\ \vdots \\ \hat{\boldsymbol{y}}^{[\rho+r]} \end{bmatrix} = \begin{bmatrix} \boldsymbol{h}(\boldsymbol{x}) \\ L_f^1 \boldsymbol{h}(\boldsymbol{x}) \\ \vdots \\ L_f^{\rho} \boldsymbol{h}(\boldsymbol{x}) \\ L_f^{\rho+1} \boldsymbol{h}(\boldsymbol{x}) \\ \vdots \\ L_f^{\rho+r} \boldsymbol{h}(\boldsymbol{x}) \end{bmatrix} + \begin{bmatrix} 0_{m\times 1} \\ \vdots \\ 0_{m\times 1} \\ \boldsymbol{H}(\hat{\bar{\boldsymbol{u}}}) \end{bmatrix} \quad (3)$$

where $\boldsymbol{H}(\hat{\bar{\boldsymbol{u}}}) \in \mathbb{R}^{m(r+1)}$ is a matrix valued function of $\hat{u}(t), \dot{\hat{u}}(t), \cdots, \hat{u}^{[r]}(t)$, given by

$$\boldsymbol{H}(\hat{\bar{\boldsymbol{u}}}) = \begin{bmatrix} L_g L_f^{\rho-1} \boldsymbol{h}(\boldsymbol{x}) \hat{\boldsymbol{u}}(t) \\ p_{11}(\hat{\boldsymbol{u}}(t), \boldsymbol{x}(t)) + L_g L_f^{\rho-1} \boldsymbol{h}(\boldsymbol{x}) \dot{\hat{\boldsymbol{u}}}(t) \\ \vdots \\ p_{r1}(\hat{\boldsymbol{u}}(t), \boldsymbol{x}(t)) + p_{r2}(\hat{\boldsymbol{u}}(t), \dot{\hat{\boldsymbol{u}}}(t), \boldsymbol{x}(t)) + \cdots \\ + \mathrm{p}_{rr}(\hat{\boldsymbol{u}}(t), \cdots, \hat{\boldsymbol{u}}^{[r-1]}(t), \boldsymbol{x}(t)) + L_g L_f^{\rho-1} \boldsymbol{h}(\boldsymbol{x}) \hat{\boldsymbol{u}}^{[r]}(t) \end{bmatrix} \quad (4)$$

$$\hat{\bar{\boldsymbol{u}}} = \left[\hat{\boldsymbol{u}}(t)^{\mathrm{T}} \quad \dot{\hat{\boldsymbol{u}}}(t)^{\mathrm{T}} \quad \ddot{\hat{\boldsymbol{u}}}(t)^{\mathrm{T}} \quad \cdots \quad \hat{\boldsymbol{u}}^{[r]}(t)^{\mathrm{T}} \right] \quad (5)$$

Within the moving time frame, the output $\hat{y}(t+\tau)$ at the time τ is approximately predicted by

$$\hat{\boldsymbol{y}}(t+\tau) \doteq \boldsymbol{\Gamma}(\tau) \hat{\bar{\boldsymbol{Y}}}(t) \quad (6)$$

where

$$\boldsymbol{\Gamma}(\tau) = \left[\boldsymbol{I}, \bar{\boldsymbol{\tau}}, \cdots, \frac{\bar{\boldsymbol{\tau}}^{(\rho+r)}}{(\rho+r)!} \right]$$

$$\bar{\boldsymbol{\tau}} = \mathrm{diag}\{\tau, \cdots, \tau\}$$

$$\bar{\tau} \in \mathbb{R}^{m\times m}, \boldsymbol{\Gamma}(\tau) \in \mathbb{R}^{m\times m(\rho+r+1)}$$

Similarly, in the moving time, the reference $\boldsymbol{w}(t+\tau)$ at the time τ is approximated by the Taylor series expansion of $\boldsymbol{w}(t)$ at the time t up to $(\rho+r)$ order, given by

$$\hat{\boldsymbol{w}}(t+\tau) \doteq \boldsymbol{\Gamma}(\tau) \overline{W}(t) \quad (7)$$

where

$$\bar{\boldsymbol{W}}(t) = \left[\boldsymbol{w}(t)^{\mathrm{T}} \ \dot{\boldsymbol{w}}(t)^{\mathrm{T}} \cdots \boldsymbol{w}^{[\rho+r]}(t)^{\mathrm{T}} \right]^{\mathrm{T}} \quad (8)$$

2.3 Optimal control

Predictive control problem can be reformulated as follows: at any time t, to find optimal $\hat{\bar{\boldsymbol{u}}}(t) \in \mathbb{R}^{(\rho+r+1)m}$ that make the performance Eq. (2) minimum. Based on the previous development, the optimal control law can be derived as [9]:

$$\boldsymbol{u}(t) = -(L_g L_f^{\rho-1} \boldsymbol{h}(\boldsymbol{x}))^{-1} (\boldsymbol{K}\boldsymbol{M}_{\rho} + L_f^{\rho} \boldsymbol{h}(\boldsymbol{x}) - \boldsymbol{W}^{[\rho]}(t)) \quad (9)$$

where $\boldsymbol{M}_{\rho} \in \mathbb{R}^{m\rho}$ is given by

$$\boldsymbol{M}_{\rho} = \begin{bmatrix} \boldsymbol{h}(\boldsymbol{x}) - \boldsymbol{W}(t) \\ L_f^1 \boldsymbol{h}(\boldsymbol{x}) - \boldsymbol{W}^{[1]}(t) \\ \vdots \\ L_f^{\rho-1} \boldsymbol{h}(\boldsymbol{x}) - \boldsymbol{W}^{[\rho-1]}(t) \end{bmatrix} \quad (10)$$

and $\boldsymbol{K} \in \mathbb{R}^{m\times m\rho}$ is the first m rows of the matrix $\bar{\boldsymbol{\Gamma}}_{rr}^{-1} \bar{\boldsymbol{\Gamma}}_{\rho r}^{\mathrm{T}}$ given by

$$\bar{\boldsymbol{\Gamma}}_{rr} = \begin{bmatrix} \bar{\boldsymbol{\Gamma}}_{(\rho+1,\rho+1)} & \cdots & \bar{\boldsymbol{\Gamma}}_{(\rho+1,\rho+r+1)} \\ \vdots & \ddots & \vdots \\ \bar{\boldsymbol{\Gamma}}_{(\rho+r+1,\rho+1)} & \cdots & \bar{\boldsymbol{\Gamma}}_{(\rho+r+1,\rho+r+1)} \end{bmatrix} \quad (11)$$

$$\bar{\boldsymbol{\Gamma}}_{\rho r} = \begin{bmatrix} \bar{\boldsymbol{\Gamma}}_{(1,\rho+1)} & \cdots & \bar{\boldsymbol{\Gamma}}_{(1,\rho+r+1)} \\ \vdots & \ddots & \vdots \\ \bar{\boldsymbol{\Gamma}}_{(\rho,\rho+1)} & \cdots & \bar{\boldsymbol{\Gamma}}_{(\rho,\rho+r+1)} \end{bmatrix} \quad (12)$$

$$\bar{\boldsymbol{\Gamma}}_{(i,j)} = \frac{\bar{\boldsymbol{\Gamma}}^{i+j-1}}{(i-1)!(j-1)!(i+j-1)} \quad (13)$$

where $i, j = 1, \cdots, \rho+r+1$, $\bar{\boldsymbol{T}} = \mathrm{diag}\{T, \cdots, T\} \in \mathbb{R}^{m\times m}$.

3 System model and controller design

3.1 System model

To study the SVC damping effect on the dynamic behavior of a power system, let us investigate a single machine system with SVC, and the equivalent circuit for the investigation is shown in Fig. 1, where the generator is represented by the classical model in which the magnitude of E_q' and the mechanical input power P_m are constant.

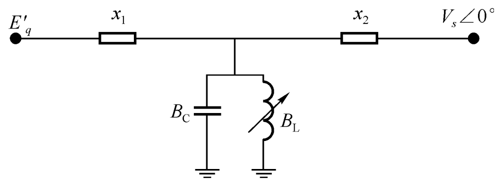

Fig. 1 Equivalent circuit of one machine infinite bus

The motion equations of the generator can be written as

$$\begin{aligned} \dot{\delta} &= \Delta\omega \\ \Delta\dot{\omega} &= -\frac{D}{H}\Delta\omega + \frac{\omega_0}{H}(P_m - P_e) \end{aligned} \tag{14}$$

where δ is power angle of the generator (in rad); $\Delta\omega$ is relative angular speed (in rad/s); $\omega_0 = 2\pi f_0$ is the synchronous angular speed; P_m, P_e are the mechanical and electromagnetic power of the generator, respectively; D the per unit damping constant; H the per unit inertia constant.

If we neglect the electromagnetic transient period of the transmission line and SVC devices, we can obtain:

$$P_e = \frac{E' V_s}{x_1 + x_2 - x_1 x_2 B_{SVC}} \sin\delta \tag{15}$$

3.2 The design principle of the controller

The conventional pure voltage regulation for SVC has been examined in terms of synchronizing torque improvement and voltage maintenance at the SVC location bus, but it will not succeed in providing the required damping after stabilization. To obtain the required damping, the control strategy for SVC should consist of a normal voltage regulation and an auxiliary damping controller as shown in Fig. 2.

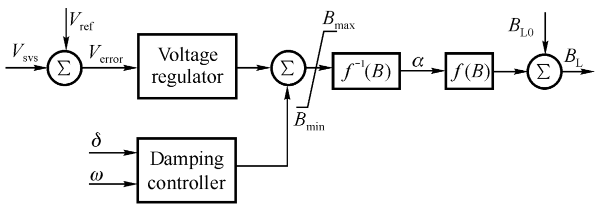

Fig. 2 Unified model for SVC

$$f(\alpha) = B_{L\max}\frac{2\pi - 2\alpha + \sin 2\alpha}{\pi} \tag{16}$$

where α is thyristor firing angle and $B_{L\max}$ is the maximum value of thyristor-controlled reactor (TCR). The conventional voltage regulator model 1 in Ref. [10] is adopted, as shown in Fig. 3

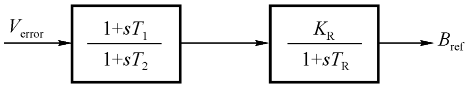

Fig. 3 Voltage regulator model

3.3 Design of damping controller based on NOPC

Equation (15) substitute in Eq. (14), it can be rewritten in affine nonlinear system as follows:

$$\begin{bmatrix} \dot{\delta} \\ \Delta\dot{\omega} \end{bmatrix} = \begin{bmatrix} \Delta\omega \\ -\dfrac{D}{H}\Delta\omega + \dfrac{\omega_0}{H}P_m \end{bmatrix} + \begin{bmatrix} 0 \\ -\dfrac{E_q' V_s \omega_0}{H}\sin\delta \end{bmatrix} u \tag{17}$$

Let

$$u = \frac{1}{x_1 + x_2 - x_1 x_2 B_{SVC}} \tag{18}$$

3.3.1 The output function choice

During post-fault in power system, we expect that the power system can get to a stable state fleetly, namely, $\Delta\omega = 0$. In other words, the reference signal would be zero if we set up output vector as follows:

$$\boldsymbol{y}(t) = \boldsymbol{h}(\boldsymbol{x}) = \Delta\omega \tag{19}$$

3.3.2 Damping module design of SVC controller based on NOPC

If we do not consider the governor's effect, from Eqs. (17)–(19), we can obtain

$$L_f \boldsymbol{h}(\boldsymbol{x}) = \frac{\partial \boldsymbol{h}(\boldsymbol{x})}{\partial \boldsymbol{x}} \boldsymbol{f}(\boldsymbol{x}) = -\frac{D}{H}\Delta\omega + \frac{\omega_0}{H}P_m \tag{20}$$

$$L_g \boldsymbol{h}(\boldsymbol{x}) = \frac{\partial \boldsymbol{h}(\boldsymbol{x})}{\partial \boldsymbol{x}} \boldsymbol{g}(\boldsymbol{x}) = -\frac{E' V_s \omega_0}{2H}\sin\delta \tag{21}$$

As Ref. [8], we can obtain that output $\boldsymbol{y}(t)$ has relative degree $\rho = 1$. Let control order $r = 0$, from Eqs. (10)–(13), we can obtain

$$\bar{\Gamma}_{rr} = T_{(2,2)} = \frac{T^3}{3} \tag{22}$$

$$\bar{\Gamma}_{\rho r} = \frac{T^2}{2} \tag{23}$$

$$\boldsymbol{K} = \bar{\Gamma}_{rr}^{-1}\bar{\Gamma}_{\rho r}^{T} = \frac{3}{2T} \tag{24}$$

$$\boldsymbol{KM}_{\rho} = \frac{3}{2T}\Delta\omega \tag{25}$$

From Eq. (9), the control law of the damping controller for SVC based on NOPC can be derived as follows:

$$u(t)=\frac{H}{\omega_0 E_q^{'} V_s \sin\delta}(\boldsymbol{KM}_\rho - \frac{D}{H}\Delta\omega + \frac{\omega_0}{H}P_{m0}) \tag{26}$$

From Eq. (18), we can obtain

$$B_L = \frac{1}{x_1 x_2}\left[\frac{\omega_0 E_q^{'} V_s \sin\delta}{H(KM_\rho) - D\Delta\omega + \omega_0 P_{m0}} - (x_1 + x_2)\right] + B_C \tag{27}$$

4 Simulation results

In this section, employing transient security assessment tool (TSAT) of DSA power tools by Powertech Labs Inc., a single machine infinite bus power Ref. [11] shown in Fig. 4 is chosen to demonstrate the effects of the controller.

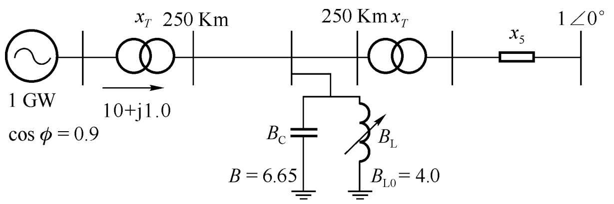

Fig. 4 Diagram of simulated system

All parameters of the study power system are in per unit value (Base value: 500 kV, 100 MVA)

Generator:

$x_d = 0.144, x_d' = 0.022\,5, x_q = 0.139\,5, D = 12.8,$

$T_{d0}' = 8.0(s), H = 66.67(s);$

Transmission line:

$r_L = 0.001\,8, x_L = 0.037\,3, B = 2.422,$

$x_s = 0.001, x_T = 0.014\,2;$

About parameters of the controller, we let control order $r = 0$ and predictive time $T = 0.1$ s.

The fault we consider in this paper is a three-phase short circuit fault and is described as follows:

At $t = 0.5$ s, a fault occurs at the high voltage bus of the transformer. At $t = 0.6$ s, the fault is cleared.

Simulation results under traditional control scheme and the proposed control scheme are shown in Fig. 5.

From the simulation curves in Fig. 5, we can find that the oscillation of the power system can be rapidly attenuated and the system can fleetly get to equilibrium point under the voltage regulator with NOPC damping control compared with the conventional pure voltage regulator. It is evident that the proposed damping controller can effectively improve the dynamic stability of the system and the SVC location bus voltage can fleetly get to a given original equilibrium point (Fig. 5(c)). Of course, voltage overshoot at the SVC location bus is slightly bigger at the initiation stage of the transient

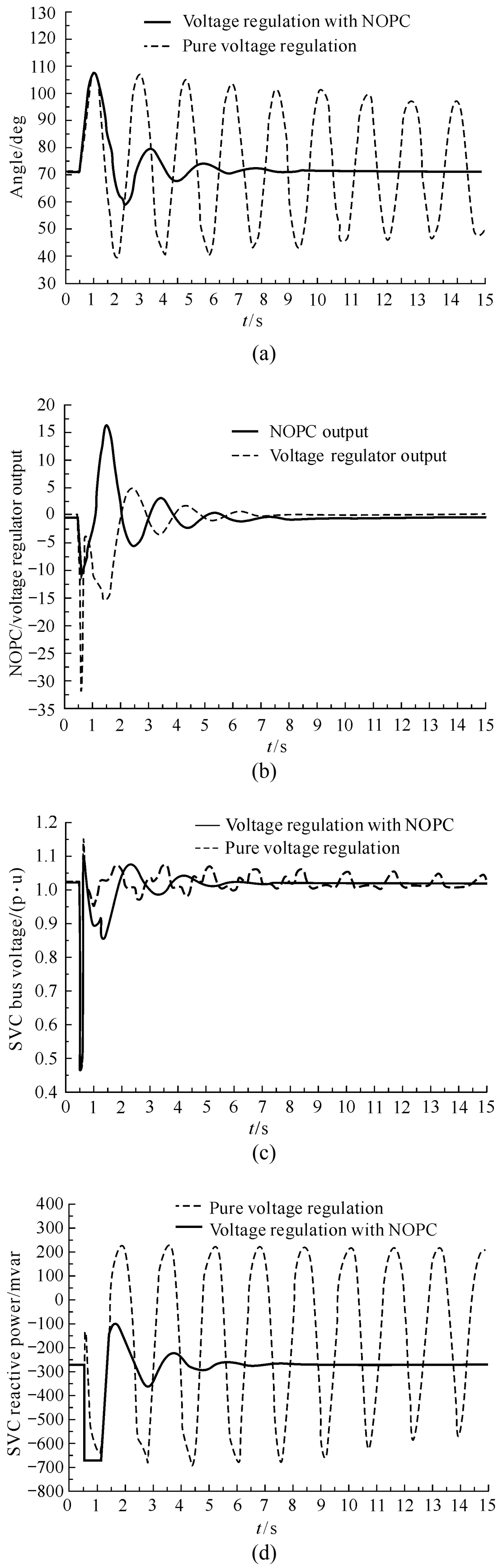

Fig. 5 System response to three-phase short circuit

process. This shows that to obtain sufficient damping and to get good voltage dynamic performance is a conflict control objective. However, it is worthy for the purpose of getting sufficient system damping by suffering moderately voltage overshoot. From Fig. 5(b), we can see that there is evidence of phase differences between the output signal of the damping control loop and of the voltage control loop during the system oscillation.

5 Conclusions

In order to improve power system damping and to maintain the voltage at the SVC location bus simultaneously, a novel design method for SVC damping controller with closed-form analytic solution control law is presented in this paper, on the basis of the nonlinear optimal predictive control theory. The merits of this damping controller can be concluded as the follows:

1) The repetition of online optimization based on real-time feedback signals can obtain continuous correct predictive control results by introducing uncertain information into the controller; hence it exhibits excellent robustness.

2) Deriving closed-form analytic solution control law, online optimization is not necessary; thus the huge calculation burden can be avoided and the demand of real-time control can be satisfied.

3) The design parameters, predictive period T and control order r, are transparent and its engineering implement is easy.

4) The stability of the closed-loop system is guaranteed.

The simulation results illustrate that the controller can fleetly attenuate power system oscillation and effectively maintain voltage at the SVC location bus.

Acknowledgements This study was supported by the National Natural Science Foundation of China (No. 50307007).

References

1. Sebastiao E. M., de Oliveira, Synchronizing and damping torque coefficients and power system steady-state stability as affected by static var compensators, IEEE Trans. Power Systems, 1994, 9(1): 109–119
2. Hammad A. E., Analysis of power system stability enhancement by static var compensators, IEEE Trans. Power Systems, 1986, 1(4): 222–227
3. Zhou E. Z., Application of static var compensators to increase power system damping, IEEE Trans. Power Systems, 1993, 8(2): 655–661
4. Li Chun, Jiang Qi-rong, Wang Zhong-hong, Design of nonlinear controller for SVC to damp power system oscillations as well as regulate voltage, Automation of Electric Power Systems, 1998, 22(6): 35–42 (in Chinese)
5. Lu Qiang, Sun Yuan-zhang, Nonlinear control of power systems, Beijing: Science Press, 1993 (in Chinese)
6. Peng Jian-chun, Huang Chun, Wang Yao-nan, Intelligent adaptive PID controller design for static var compensator, Journal of Hunan University (Natural Sciences Edition), 1999, 26(5): 50–55 (in Chinese)
7. Sun Hao, Xi Yu-geng, Zhang Zhong-jun. Model predictive control algorithm for a class of nonlinear systems, Journal of Shanghai Jiao Tong University, 1994, 28(4): 68–75 (in Chinese).
8. Isidori A., Nonlinear control systems: an introduction, 3rd, Berlin: Spring-Verlag, 1995
9. Chen Wen-hua, Donald J. Balance, Peter J. Gawthrop, Optimal control of nonlinear systems: a predictive control approach, Automatica, 2003, 39(4): 633–641
10. IEEE Special Stability Controls Working Group, Static var compensator models power flow and dynamic performance simulation, IEEE Trans. Power Systems, 1994, 9(1): 229–240
11. Ma You-jie, The nonlinear control of SVC cooperate with the excitation system of generator, Transactions of China Electrotechnical Society, 1998, 13(4): 1–4 (in Chinese)